



Universiteit  
Leiden  
The Netherlands

## **In situ imaging reveals properties of purinergic signalling in trigeminal sensory ganglia in vitro**

Nowodworska, A.; Maagdenberg, A.M.J.M. van den; Nistri, A.; Fabbretti, E.

### **Citation**

Nowodworska, A., Maagdenberg, A. M. J. M. van den, Nistri, A., & Fabbretti, E. (2017). In situ imaging reveals properties of purinergic signalling in trigeminal sensory ganglia in vitro. *Purinergic Signalling*, 13(4), 511-520. doi:10.1007/s11302-017-9576-1

Version: Not Applicable (or Unknown)

License: [Leiden University Non-exclusive license](#)

Downloaded from: <https://hdl.handle.net/1887/94914>

**Note:** To cite this publication please use the final published version (if applicable).

# In situ imaging reveals properties of purinergic signalling in trigeminal sensory ganglia in vitro

Arletta Nowodworska<sup>1</sup> · Arn M. J. M. van den Maagdenberg<sup>2</sup> · Andrea Nistri<sup>1</sup> · Elsa Fabbretti<sup>3,4</sup>

Received: 8 January 2017 / Accepted: 1 August 2017 / Published online: 18 August 2017  
© Springer Science+Business Media B.V. 2017

**Abstract** Chronic pain is supported by sterile inflammation that induces sensitisation of sensory neurons to ambient stimuli including extracellular ATP acting on purinergic P2X receptors. The development of in vitro methods for drug screening would be useful to investigate cell crosstalk and plasticity mechanisms occurring during neuronal sensitisation and sterile neuroinflammation. Thus, we studied, at single-cell level, membrane pore dilation based on the uptake of a fluorescent probe following sustained ATP-gated P2X receptor function in neurons and non-neuronal cells of trigeminal ganglion cultures from wild-type (WT) and R192Q *Ca<sub>v</sub>2.1* knock-in (KI) mice, a model of familial hemiplegic migraine type 1 characterised by neuronal sensitisation and higher release of soluble mediators. In WT cultures, pore responses were mainly evoked by ATP rather than benzoyl-ATP (BzATP) and partly inhibited by the P2X antagonist TNP-ATP. P2X7 receptors were expressed in trigeminal ganglia mainly by non-neuronal cells. In contrast, KI cultures showed higher expression of P2X7 receptors, stronger responses to BzATP, an effect largely prevented by prior administration of *Ca<sub>v</sub>2.1* blocker  $\omega$ -agatoxin IVA, small interfering RNA (siRNA)-based

silencing of P2X7 receptors or the P2X7 antagonist A-804598. No cell toxicity was detected with the protocols. Calcitonin gene-related peptide (CGRP), a well-known migraine mediator, potentiated BzATP-evoked membrane permeability in WT as well as R192Q KI cultures, demonstrating its modulatory role on trigeminal sensory ganglia. Our results show an advantageous experimental approach to dissect pharmacological properties potentially relevant to chronic pain and suggest that CGRP is a soluble mediator influencing purinergic P2X pore dilation and regulating inflammatory responses.

**Keywords** Pain · Migraine · P2X3 · P2X7 · DRG · ATP · *CACNA1A* · FHM1

## Abbreviations

$\alpha, \beta$ -meATP	$\alpha, \beta$ -methyleneATP
Aga	$\omega$ -Agatoxin IVA
AU	Arbitrary units
CGRP	Calcitonin gene-related peptide
KI	Knock-in
TG	Trigeminal ganglion
Vs	Versus
WT	Wild-type
AU	arbitrary units

**Electronic supplementary material** The online version of this article (doi:10.1007/s11302-017-9576-1) contains supplementary material, which is available to authorized users.

✉ Elsa Fabbretti  
e.fabbretti.bf@gmail.com

<sup>1</sup> Neuroscience Department, International School for Advanced Studies (SISSA), Via Bonomea 265, 34136 Trieste, Italy

<sup>2</sup> Departments of Human Genetics & Neurology, University Medical Centre, Einthovenweg 20, 2333 ZC Leiden, Netherlands

<sup>3</sup> Center for Biomedical Sciences and Engineering, University of Nova Gorica, Vipavska 13, 5000 Nova Gorica, Slovenia

<sup>4</sup> Present address: Department of Life Sciences, University of Trieste, via Giorgieri 5, 34127 Trieste, Italy

## Introduction

Chronic pain is characterised by abnormal crosstalk between neuronal and non-neuronal cells governed by altered levels of soluble inflammatory pain mediators, such as cytokines, calcitonin gene-related peptide (CGRP) and ATP [1]. These mediators result in neuronal sensitisation due to persistent changes in ganglion environment, inducing tissue remodelling and creating new

pharmacological properties via new receptor synthesis and assembly, cell recruitment and neuroinflammation. Recent evidence suggests that in chronic pain, ATP-gated P2X receptors play a pivotal role in triggering and supporting these phenomena [2, 3]. Considering the heterogeneous expression of ATP-gated receptors in neurons and non-neuronal cells [4, 5], the outcome of purinergic signalling is likely to depend on the time course of receptor activity, in turn related to the tissue context and the molecular mechanisms at the single-cell level. In particular, when persistently exposed to an agonist, certain P2X receptors induce reversible changes in cell membrane permeability characterised by emergence of large pores through which even large size molecules can permeate [6, 7]. Although the underlying biophysical mechanisms are not fully understood, this transient increase in membrane permeability was first shown for P2X7 receptors [8] and later for P2X2 and P2X4 receptors [9, 10]. The current hypothesis is that this process may be essential for sustaining acute inflammation and its further amplification. Interestingly, pore dilation can be measured at the single-cell level because the strong permeability enables measurement of inflow of fluorescent probes [10]. Furthermore, expression and function of pore-forming receptors in different conditions may vary as outcome of different pathophysiological conditions and molecular mechanisms [11].

Our previous work was concerned with R192Q  $Ca_v2.1$  knock-in mice (R192Q KI), which express voltage-gated  $Ca_v2.1$   $Ca^{2+}$  channels containing  $\alpha_{1A}$  subunits harbouring the R192Q missense mutation that leads to familial hemiplegic migraine type 1 (FHM-1) in patients [12, 13]. This model suggests a direct link between mutated  $Ca_v2.1$  channels, potentiated neuronal responses and an inflammatory basal state [14, 15] due to a larger release of CGRP [16], ATP and TNF- $\alpha$  [17, 18]. The present study aimed at comparing the occurrence, time course and intensity of responses of wild-type (WT) and R192Q KI trigeminal ganglion (TG) cultures. To this end, we decided to use an experimentally advantageous approach based on fluorescence imaging at the single-cell level rather than measuring the average fluorescent intensity of a cell population. In fact, within a heterogeneous cell population like the one employed in the present study, our method based on pore permeability evoked by ATP-receptor agonists enabled us to identify responsive cells on the basis of their morphology and, thus, to investigate cell-cell crosstalk elicited by different pharmacological treatments over time.

## Methods

### Primary cultures

The mouse model of FHM-1, namely the R192Q KI [13], and their WT littermates were used. All animal procedures were in accordance with national regulations of animal welfare and

approved by the ethics committee of the International School for Advanced Studies (SISSA). Genotyping was performed by PCR as previously reported [13]. Primary cultures of TG ganglia from mice of 12–14 days were prepared as previously described [14] and used 24 h after plating. For small interfering RNA (siRNA) experiments, TG cultures were transfected 24 h after plating with SMARTpool mouse siP2X7 (5'-GGAAAGAGCCUGUUAUCAG-3', 5'-UAGCAGAGGUGACGGAGAA-3', 5'-UACAUUAGCUUUGCUUUGG-3', 5'-GGAUCCAGAGCACGAAUUA-3'; GE Healthcare Dharmacon Inc., Chicago, IL, USA) and used 48 h later. In each experiment, control cultures were transfected with scramble RNA and siGLO RISC-free siRNA (GE Healthcare Dharmacon Inc.) and used to compare responses with treated cultures.

### Pore permeability fluorescence assay

Time-lapse in situ imaging of membrane permeability was performed according to standard protocols [6]. Briefly, TG cultures (plated on 18-mm glass slides) were incubated with ethidium bromide (EtBr; 5  $\mu$ g/mL; Sigma-Aldrich, S. Giuliano Milanese, Italy) for 5 min at room temperature in HBSS buffer (152 mM NaCl, 5 mM KCl, 1 mM  $MgCl_2$ , 2 mM  $CaCl_2$ , 10 mM glucose, 10 mM HEPES; pH 7.4). ATP (0.01, 0.1 or 1 mM), the non-hydrolysable ATP analog  $\alpha,\beta$ -methylene ATP ( $\alpha,\beta$ -meATP; 100  $\mu$ M) and the P2X7 receptor agonist 2',3'-O-(4-benzoylbenzoyl)-ATP (BzATP; 300  $\mu$ M) were obtained from Sigma-Aldrich and were added to the cultures to evoke membrane permeability and EtBr uptake. In certain experiments, TG cultures were pre-incubated (15 min) with the P2X antagonist TNP-ATP (25  $\mu$ M, Sigma-Aldrich;  $IC_{50}[P2X7] > 30 \mu$ M) [5]; P2X7 receptor antagonist A-804598 (100 nM; Tocris Biosciences, Bristol, UK;  $IC_{50}[P2X7] = 100$  nM) [19]; or the P/Q-type  $Ca_v2.1$ -specific channel blocker  $\omega$ -agatoxin IVA (400 nM; 15 h; Tocris Biosciences) [14]. Control experiments were performed in parallel on the same day and used for statistical comparison.

Cytotoxicity developing during the pore permeability fluorescence assay [20] was quantified by counting pyknotic cells in control conditions and after 1 or 24 h from 1-h-long stimulation with ATP (1 mM) or BzATP (300  $\mu$ M) as shown in Suppl. Fig. 1 a, b ( $n = 3$ ).

Fluorescence microscopy images (rate 1/min) were acquired for a total of 40 min in time-lapse mode with a Nikon Eclipse Ti fluorescence microscope and Nikon Elements software (Nikon Instruments Europe, Amsterdam, The Netherlands). For post-acquisition analysis of morphologic parameters and cell counting of neuronal and non-neuronal responding cells, each recording was accompanied by two series of phase-contrast and fluorescence microscopy images acquired at the beginning and the end of the recording (as exemplified in Suppl. Fig. 2a, b). Nuclear labelling with fluorescent probe Hoechst 33342

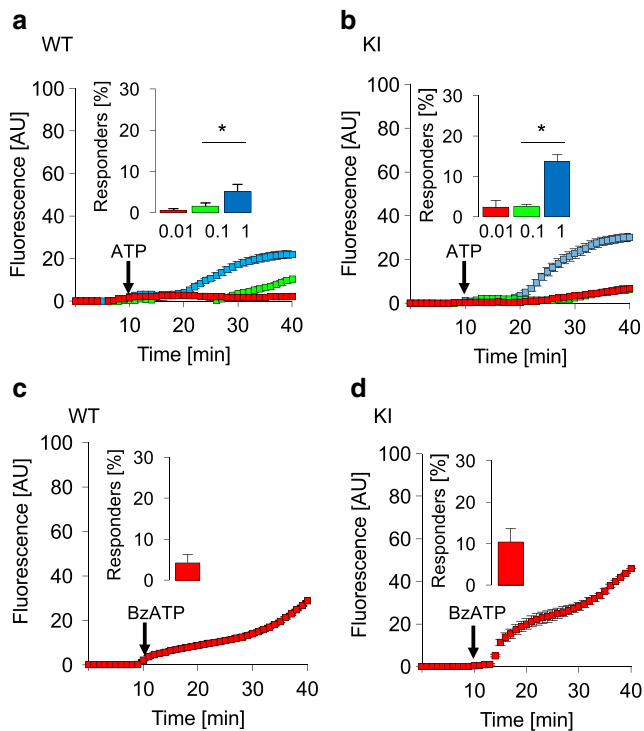


**Fig. 1** Fluorescence recordings of membrane pore permeability in TG cultures. **a, b** Imaging recordings of EtBr fluorescence intensity (in arbitrary units, AU) of TG cultures from WT (**a**) or R192Q KI mice (**b**), to quantify the membrane pore permeability at the single-cell level during the time (min) after application of ATP (0.01, 0.1 or 1 mM, as indicated). ATP was applied after 10 min from the beginning of the recordings (arrows). In insets, histograms quantify the percent of responding cells in each condition, counted on the total number of cells after 20 min from the beginning of the recordings. For WT:  $n = 3–6$  experiments; with 919, 2711 or 2812 analysed cells for 0.01, 0.1 or 1 mM ATP, respectively. For KI:  $n = 3–4$ ; with 1068, 557 or 535 analysed cells for 0.01, 0.1 or 1 mM ATP, respectively;  $*p = 0.001$  (0.1 vs 1 mM ATP, both for WT and KI samples). **c, d** As before, after application of BzATP (300  $\mu$ M, arrows);  $n = 5$ , for a total of 6825 analysed cells for WT and 3782 for KI samples

identified single cells in which a region of interest (ROI) was used to quantify fluorescence intensity in arbitrary units (AU) with ImageJ software (time-series analyser module; NIH, Bethesda, MA, USA). Since the basal rise in ROI fluorescence was linear (in the absence of agonists, F0; Suppl. Fig. 2c), in each experiment, fluorescence values during the first 10 min were used to extrapolate the slope of the basal time/fluorescence plot (as shown in Suppl. Fig. 2d) subsequently subtracted from the data shown in Figs. 1, 2, 4, 5 and 6. Average of single-cell fluorescence intensity values ( $F_m$ ) evoked by the agonists was then normalised to baseline values ( $F_m - F_0$ ) and plotted as function of time ( $F_m - F_0/\text{min}$ ) using Microsoft Office Excel. The percentage of responding cells was calculated as the number of responding ROIs over the total number of nuclei (probed with Hoechst 33342), counted at the end of the recording (taken as 100%). Summary of the number of analysed cells is included in figure legends, Tables 1 and 2 and Suppl. Tables 1 and 2.

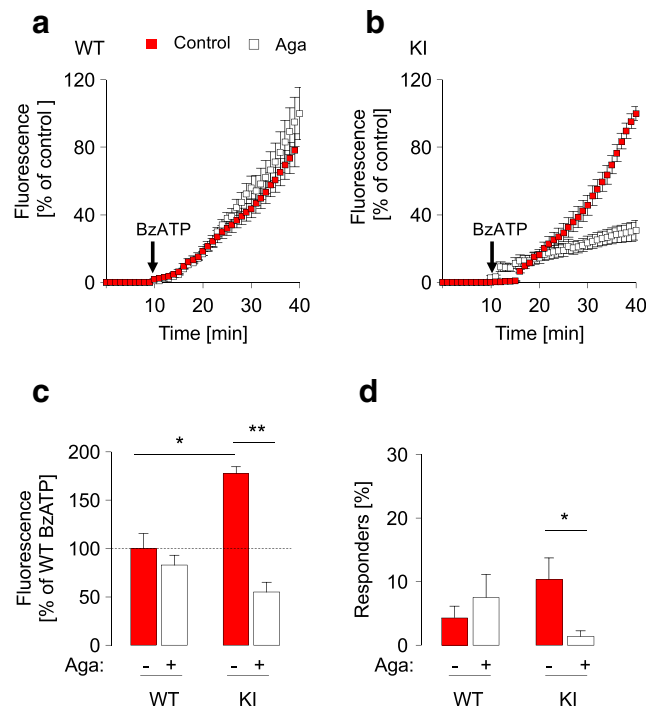


**Fig. 2** Effect of  $\omega$ -agatoxin IVA on membrane pore permeability evoked by BzATP. **a, b** Membrane pore permeability of TG cultures from WT (**a**) or R192Q KI mice (**b**) after application of BzATP (300  $\mu$ M) alone or after pre-treatment with  $\omega$ -agatoxin IVA (Aga; 400 nM, 15 h). Data are expressed as percent of mean of maximum fluorescence intensity values of untreated control culture after application of BzATP (300  $\mu$ M, 30 min);  $n = 3$ . **c** Histograms quantify the fluorescence intensity (expressed as % of response of WT untreated control cultures at 40 min, taken as 100%, dashed line) in WT and KI cultures, in standard control conditions or after pre-treatment with Aga (400 nM, 15 h) as indicated;  $n = 3$ ,  $*p = 0.003$  (WT vs KI),  $**p = 0.001$  (KI vs KI Aga). **d** Percent of responding cells counted after 20 min from beginning of the recording experiments, calculated on a total of 377 WT and 322 KI cells;  $n = 3$ ;  $*p = 0.004$  (KI vs KI Aga)

## Immunofluorescence experiments

TG ganglia and cultures were processed for immunofluorescence as previously described [14] with minimal modifications. Samples were incubated with a blocking buffer composed by 10% horse serum and 0.1% Triton X-100 in phosphate buffer for 1 h and incubated with anti-P2X7 antibodies (1:500; Alomone Labs, Jerusalem, Israel), anti-glutamine synthase (1:150; Millipore, Milan, Italy), anti-CD11b (1:100, Sigma-Aldrich), F4/80 antibodies (1:100, Sigma-Aldrich) and anti- $\beta$ -tubulin 3 (1:1000; Sigma-Aldrich) antibodies for 2 h at room temperature in the same buffer. Signal was detected with AlexaFluor 488- or 594-conjugated secondary antibodies (1:500; ThermoFisher Scientific Inc.). Immunofluorescence experiments with anti-P2X7 receptors (1:100; Alomone) were tested for specificity in mouse macrophage cell line J774.2 and in P2X7-negative HEK293 cells

**Table 1** Fluorescence responses of WT and R192Q KI TG cultures to ATP

ATP	WT 0.01 mM	KI	WT 0.1 mM	KI	WT 1 mM	KI
% responders <sub>[20 min]</sub>	0.5 ± 0.48	2.4 ± 0.75	1.5 ± 0.8	2.5 ± 0.5	5.1 ± 1.4	13.6 ± 0.7***
Fluorescence intensity 20 min	2.6 ± 0.5	0.5 ± 0.3	0 ± 0.5*	1.7 ± 0.06*	4 ± 0.4	3.3 ± 1
Fluorescence intensity 40 min	3.2 ± 1.9	6.5 ± 2.9	10.4 ± 1.7	7.4 ± 1.3	19.1 ± 1.5	33.7 ± 1.7**
Rate	0.4	0.3	0.7	0.3	1.3	1.7
Latency	37	19.8	25	21	17	19.4
Time-to-peak/to-plateau	55	55	55	30	30	31
No. experiments	3	3	6	4	6	4
Total no. of cells	919	1068	2711	557	2812	535

Intensity is measured after 20 or 40 min from the beginning of the recordings or at peak and is expressed as AU values. Latency to a response, rate, time-to-peak and time-to-plateau are expressed in minutes

\* $p = 0.001$  (0.1 mM vs 1 mM ATP, both for WT and KI samples); \*\* $p = 0.043$  (1 mM WT vs KI); \*\*\* $p = 0.001$  (%WT vs KI responding cells, tested with 1 mM ATP)

(Suppl. Fig. 2e). Nuclei were counterstained with Hoechst 33342 (1:1000; Sigma-Aldrich). Samples were mounted on glass slides with anti-fading reagent (Vector Laboratories, Burlingame, CA, USA) and analysed with the Nikon fluorescence microscope.

### Western blot

Efficiency of siP2X7 in TG cultures was measured by Western blotting. Forty-two hours after application of siRNA (72 h after plating), protein extracts were prepared from TG cultures in 30 mM Tris-HCl (pH 7.5), 150 mM NaCl and 1% CHAPS plus protease inhibitors (Sigma-Aldrich). Extracts were kept on ice for 30 min and centrifuged at 6000×*g* for 5 min. Twenty micrograms of protein extract was loaded on a SDS-polyacrylamide gel (10%) and transferred to nitrocellulose

membranes. Membranes were incubated with anti-P2X7 antibodies (1:500; Alomone Labs). Signals were detected with an enhanced chemiluminescence light system (ECL; Amersham, Uppsala, Sweden), quantified with Alliance UVtech (Cambridge, UK) and normalised with respect to the level of β-actin (1:500; Sigma-Aldrich), which was used as gel loading control.

### Data analysis and statistics

Data are expressed as mean ± standard error of the mean (SEM), where *n* indicates the number of experiments. Statistical analysis was performed using the nonparametric Mann-Whitney rank sum test or *t* test using software directed analysis (Sigma Plot & Sigma Stat, Chicago, IL, USA). A *p* value of < 0.05 was accepted as indicative of a statistically significant difference.

**Table 2** Fluorescence responses of WT and R192Q KI TG cultures to BzATP

BzATP = 300 μM	WT	KI
% responders <sub>[20 min]</sub>	4.3 ± 0.85	10 ± 1.6***
Fluorescence intensity after 20 min	8.7 ± 1.1	20 ± 2.4*
Fluorescence intensity after 40 min	28.7 ± 6.7	46 ± 5**
Rate	0.5	1
Latency	15	10
Time to peak/plateau	55	55
No. experiments	5	5
Total no. of cells	7161	5955

Responders are expressed as percentage of total number of cells. Intensity is measured after 20 min from initial of the recording or at peak, expressed in AU values

\* $p = 0.005$  (WT vs KI); \*\* $p = 0.001$  (WT vs KI); \*\*\* $p = 0.008$  (%WT vs KI responding cells)

## Results

### ATP (or synthetic agonists) induced pore permeability change in TG cultures from WT and R192Q KI mice

Previous studies have characterised the mouse TG primary cultures [21]. In particular, while sensory neurons are a minority component either in situ or in culture, a variety of non-neuronal cells is observed that comprise a large population of macrophages, satellite glial cells and fibroblasts [4, 16, 18]. In the present experiments, we investigated the membrane permeability of TG culture cells to EtBr. In WT cultures, application of ATP (0.01, 0.1 or 1 mM, arrows in Fig. 1a) enhanced single-cell fluorescence in a dose-dependent manner. The number of ATP-responsive cells also grew in relation to the concentration of ATP and was significantly different between

0.1 and 1 mM ( $n = 4-6$ ;  $p = 0.001$ ; Fig. 1a, insets). The response latency was dependent on the ATP concentration used in the assay; on average, the latency was 25 min for 0.1 mM and 17 min for 1 mM ATP (Table 1). In R192Q KI cultures, after 20 min from beginning of the recordings, 1 mM ATP induced a stronger response than 0.1 mM ATP in WT and R192Q KI cultures ( $n = 4-6$  experiments;  $p = 0.001$ ; Fig. 1b), and the number of cells responsive to 1 mM ATP was also significantly ( $p = 0.001$ ) larger in R192Q KI cultures than WT (Table 1). The data sets of the number of responders measured after 20 min and at the end of the recording are included in Suppl. Table 1.

Although ATP is a natural agonist of P2 receptors, its ability to bind and activate a wide population of P2X and P2Y receptors makes it difficult to assess the actual receptor contribution from the obtained fluorescence signals. The P2X receptor first reported for its ability to generate pore dilation with increased membrane conductance is the P2X7 subtype. Thus, we next explored the effect of the synthetic P2X7 receptor agonist BzATP (Table 2). In WT cultures, BzATP (300  $\mu$ M) evoked a fluorescence signal that rapidly grew faster in 283 out of 6825 total analysed cells to reach a level of fluorescence intensity comparable with the one produced by 1 mM ATP in the same time interval (in 143/2812 cells; Fig. 1a, c). In R192Q KI cultures, fluorescence intensity responses to BzATP were significantly stronger already after 20 min from the beginning of the recordings ( $8.7 \pm 1.1$  in WT and  $20 \pm 2.4$  in KI,  $n = 5$ ,  $p = 0.005$ ) that further increased after 40 min ( $28.7 \pm 6.7$  in WT and  $46 \pm 5$  in KI; Fig. 1c, d and Table 2). The fluorescence uptake following BzATP application was observed in a significantly larger number of responding R192Q KI cells (389/3782 cells) than in WT (282/6825 cells;  $n = 5$ ,  $p = 0.008$ ; Fig. 1c, d, insets). The number of responding cells to BzATP was growing during the time course, as shown in Suppl. Table 1. Any cytotoxicity originating from the pharmacological treatments was quantified in control conditions and after 1 or 24 h from 1-h-long application of ATP (1 mM) or BzATP (300  $\mu$ M): data are shown in Suppl. Fig. 1a, b ( $n = 3$ ). The EtBr uptake was mainly observed in spindle-like glial cells and in flat, large inflammatory cells immunopositive for the macrophage markers F4/80 or CD11b (Suppl. Fig. 2a, b; [18]). The EtBr fluorescence uptake was observed also in a minority of neurons (15% of WT and 18% KI neurons; calculated on 659 WT and 466 KI neurons;  $n = 9-6$  experiments).

We cannot exclude that non-P2X7 receptors (like P2X2 receptors) were involved in this phenomenon. For instance, since KI cultures constitutively express potentiated P2X3 receptors [14], we applied  $\alpha, \beta$ -meATP (agonist of P2X1, P2X2/3 and P2X3 receptors [5]) and we measured the time course of pore formation (Suppl. Fig. 3). After 10 min from  $\alpha, \beta$ -meATP application (100  $\mu$ M), we observed a fluorescence signal in a small number of WT cells (6/418;  $n = 3$ ). This phenomenon was further characterised by 20 min time to plateau and substantially smaller in R192Q KI cultures, though present in a

larger number of cells (131/949;  $n = 4$ ;  $p = 0.026$ ; Suppl. Fig. 3). The number of the cells responsive to  $\alpha, \beta$ -meATP did not change further during the time course (Suppl. Table 1). These experiments demonstrated a significantly early response in a larger number of  $\alpha, \beta$ -meATP responding cells in KI with respect to WT cultures.

### The enhanced R192Q KI fluorescence profile was normalised by the P/Q-type blocker $\omega$ -agatoxin IVA

The difference in fluorescence responses between WT and R192Q KI cultures might be correlated to sensory neuron sensitisation and/or the neuroinflammatory state previously reported for R192Q KI TG cultures [14, 18]. We, therefore, tested the effect of the P/Q-type  $\text{Ca}_v2.1$  blocker  $\omega$ -agatoxin IVA (400 nM, 15 h) on fluorescence signals induced by BzATP (300  $\mu$ M).  $\omega$ -Agatoxin IVA had no significant effect on background fluorescence intensity of WT cultures nor did it change responses to BzATP (Fig. 2a, c). However, in R192Q KI cultures pre-treated with  $\omega$ -agatoxin IVA, the response to BzATP was significantly smaller compared to untreated control ( $p = 0.001$  for KI Aga vs KI control; Fig. 2b, c) and generated by a lower number of cells (4/322;  $p = 0.004$ ; Fig. 2d), while the toxin pre-incubation did not significantly alter the number of responding cells in WT cultures (24/377; Fig. 2d). These experiments suggest that responses evoked by BzATP on R192Q KI cultures were strongly up-regulated as a consequence of the R192Q  $\text{Ca}_v2.1$  channel mutation.

### P2X7 receptor expression in TG tissue and cultures from WT or R192Q KI mice

Next, we investigated whether differences between WT and R192Q KI cultures observed after application of BzATP could be attributed to differences in the expression of P2X7 receptors by employing fluorescence microscopy experiments and specific anti-P2X7 receptor antibodies, validated in control experiments (Suppl. Fig. 2e). In TG tissue in situ, P2X7 receptor immunoreactive cells were more abundant ( $p = 0.006$ ) in R192Q KI than WT mice, as the signal was mainly localised to fibre regions ( $n = 3$ ; Fig. 3a). In TG cultures, P2X7 receptor staining was observed in few non-neuronal cells (Fig. 3b) as previously reported [22–24], and the number of P2X7 positive cells was similar in R192Q KI culture and typical of satellite glial cells counterstained with glutamine synthase (Fig. 3b).

We then explored the pharmacological profile of the BzATP effect. For this purpose, we first used the broad-spectrum P2X antagonist TNP-ATP, which at 25  $\mu$ M concentration (15 min) had little effect on the response to BzATP (300  $\mu$ M) by WT or R192Q KI cultures (Fig. 4a, b), albeit the number of responsive cells was lower in R192Q KI cultures ( $n = 3$ ,  $p = 0.02$ ; Fig. 4b and Suppl. Table 2). Because

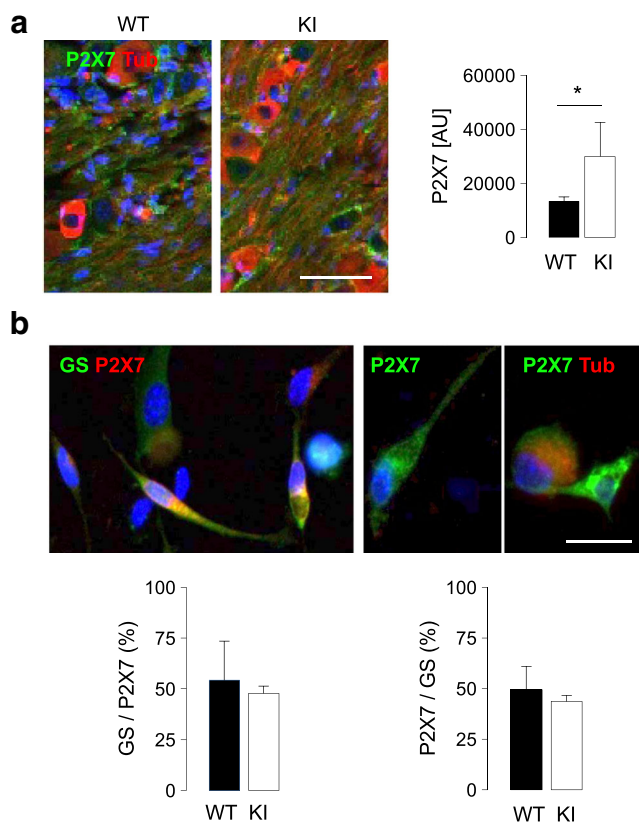


**Fig. 3** Expression of P2X7 receptors in TG ganglia and cultures. **a** Example of fluorescence microscopy photographs of TG ganglia from WT and R192Q KI mice, stained with anti-P2X7 receptors and neuron-specific anti- $\beta$ -tubulin III antibodies, as indicated. Scale bar, 50  $\mu$ m. Histograms quantify the P2X7 immunoreactivity in WT and KI TG tissue per ROI expressed in arbitrary units (AU);  $n = 3$ ;  $*p = 0.006$ . **b** Example of fluorescence microscopy photographs of R192Q KI TG cultures, stained with anti-P2X7 receptors and anti-glutamine synthase (GS) antibodies or with anti-P2X7 receptors and  $\beta$ -tubulin III antibodies. Nuclei are stained with Hoechst 33342. Scale bar, 20  $\mu$ m. Histograms quantify the percent of occurrence of P2X7 receptor immunopositive GS cells in WT and KI TG cultures which was not significantly different between the two cell samples;  $n = 3$

TNP-ATP lacks subtype receptor selectivity [5], the selective P2X7 receptor antagonist A-804598 (100 nM, 15 min; [19]) was tested next. As indicated in Fig. 4c, this antagonist had no significant effect on BzATP-induced responses in WT cultures (3.9% fluorescence intensity in WT control vs  $4.4 \pm 0.6\%$  in WT A-804598-treated cells, in 33/1312 cells; Suppl. Table 2). However, in R192Q KI cultures, A-804598 decreased the intensity signal elicited by BzATP ( $8.2 \pm 6\%$  in KI control vs 4.1% in KI A-804598-treated cells;  $n = 4$ ;  $p = 0.04$ ; Fig. 4d), a phenomenon associated with a significantly lower number of responsive cells with respect to untreated control R192Q KI samples (17/398 A-804598-treated cells;  $n = 4$ ,  $p = 0.026$ ; Fig. 4d and Suppl. Table 2).

We further studied the role of P2X7 receptor expression by siRNA silencing (siP2X7) in TG cultures (Fig. 5a, b and Suppl. Fig. 4). Under this condition, the fluorescence signal

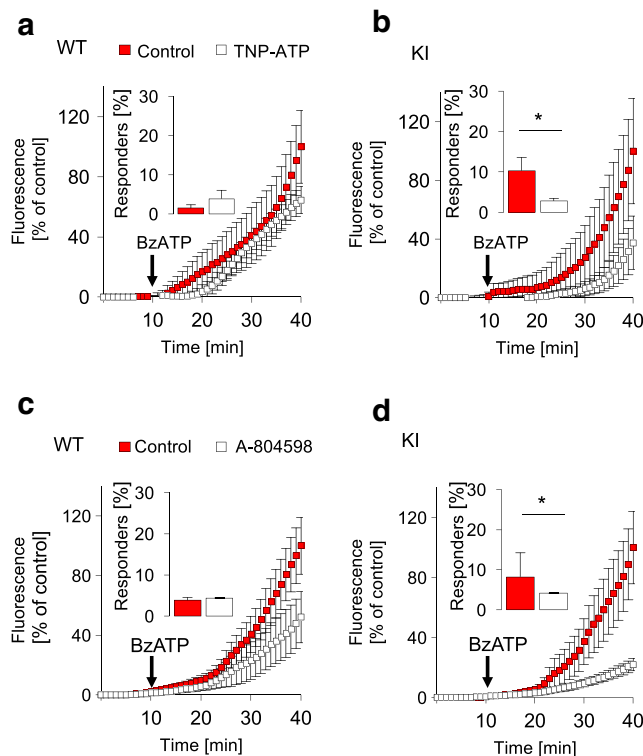


**Fig. 4** Effect of the antagonists TNP-ATP and A-804598 on pore permeability evoked by BzATP. **a, b** Fluorescence recording profiles during the time (min) in TG cultures from WT (**a**) or R192Q KI (**b**) after application of BzATP (300  $\mu$ M, arrows) alone or in cultures pre-treated with TNP-ATP (25  $\mu$ M, 15 min). Histograms (insets) quantify the percent of responding cells, measured after 20 min from beginning of the recordings, namely in 29/815 WT and 23/705 KI cells;  $n = 3$ ,  $*p = 0.016$  (KI vs KI TNP-ATP). **c, d** Fluorescence recordings quantify pore formation in TG cultures pre-treated with the P2X7 antagonist A-804598 (100 nM, 15 min);  $n = 4$ . Histograms quantify the number of responding cells after 20 min from beginning of recordings. Increased fluorescence uptake was observed in 33/1312 WT and 17/398 KI cells;  $n = 4$ ,  $*p = 0.026$  (KI vs KI A80)

evoked by BzATP (300  $\mu$ M) in WT cultures remained the same with respect to the signal recorded from cultures treated with scramble siRNA with no significant change in the number of responsive cells (48/1032 siP2X7-treated WT cells,  $n = 8$ ; Fig. 5a). In R192Q KI cultures, BzATP evoked a smaller fluorescence signal after siP2X7 application compared to control (Fig. 5b) associated with significantly lower number of cells (17/1087 siP2X7-treated KI cells;  $n = 8$ ,  $p = 0.001$ ; Fig. 5b and Suppl. Table 2), suggesting a substantial contribution of P2X7 receptors in BzATP-evoked pore formation by R192Q KI samples. We wondered whether other P2X receptor subtypes might be involved in the fluorescence responses after siP2X7. Among other pore-forming structures, P2X4 receptors were reported [6], which prompted us to perform P2X4 receptor silencing. Treatment of TG cultures with siP2X4 significantly lowered the EtBr uptake and the number of

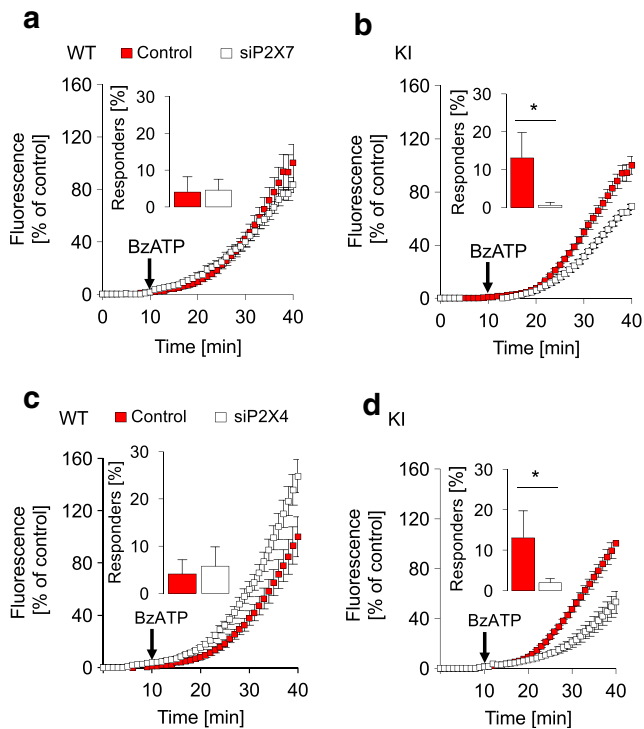


**Fig. 5** siP2X4 or siP2X7 modulates BzATP-evoked fluorescence in TG cultures. **a, b** Membrane pore permeability in TG cultures from WT (**a**) or R192Q KI (**b**) after application of BzATP (300  $\mu$ M, *arrows*), after application of scrambled siRNA (control) or siP2X7. Histograms (*insets*) quantify the percent of responding cells, measured after 20 min from beginning of recording, i.e. fluorescence uptake was measured in 48/1032 siP2X7 WT cells and in 17/1087 siP2X7 KI cells;  $n = 5$ ,  $*p = 0.001$  (KI vs KI siP2X7). **c, d** Membrane pore permeability in TG cultures from WT (**c**) or R192Q KI (**d**) after application of BzATP (300  $\mu$ M, *arrows*), after application of scrambled siRNA (control) or siP2X4. Histograms quantify the percent of responding cells after 20 min from beginning of the recordings, corresponding to 10/297 WT and 11/502 KI cells;  $n = 3$ ,  $*p = 0.027$  (KI vs KI siP2X4)

responding cells with respect samples treated with scramble siRNA (10/297 in WT and 11/502 in KI siP2X4-treated cells;  $n = 3$ ,  $*p = 0.027$ ; Fig. 5c, d).

### Functional relevance for migraine mediator signalling

Among different pain mediators, CGRP has been identified as a major contributor to migraine pain [25]. In fact, ambient CGRP concentrations are almost doubled in R192Q KI cultures with respect to WT and membrane depolarisation evokes release of CGRP more than five times larger by R192Q KI cultures than by WT ones [16]. CGRP also potentiates P2X3-mediated neuronal responses and P2Y receptor-mediated responses in satellite glial cells of TG ganglia [16, 26]. In order to test whether CGRP may influence fluorescence responses triggered by BzATP (300  $\mu$ M), TG cultures were pre-treated with CGRP (1  $\mu$ M, 4 h) before testing. In WT and R192Q KI cultures, this treatment significantly potentiated the fluorescence signal ( $p = 0.01$ ; Fig. 6a, b), an effect readily observed in WT and KI cultures (Fig.

6c). In addition, in WT samples treated with CGRP, 68/376 cells responded to BzATP with pore formation at early time points, a number that did not grow further (Suppl. Table 2). In R192Q KI samples, CGRP induced a delayed rise in the number of responding cells (from 52 at early stages to 81 responders at end points out of a total of 496 KI cells). Application of the CGRP receptor blocker CGRP<sub>8–37</sub> strongly reduced the number of pore forming cells in R192Q KI cultures (63/597 WT cells vs 15/793 KI cells; Fig. 6d) in line with the larger constitutive release of CGRP by this model.

## Discussion

In the present study, we applied the membrane permeability assay to interrogate the cell-to-cell crosstalk based on activation of purinergic receptors in primary TG cultures. Notably, fluorescent probe uptake, measured in a time-lapse mode at the single-cell level, provided a useful monitoring of the dynamics of evoked responses. The different activation profiles detected in WT and R192Q KI cultures supported the previously demonstrated alteration in neuro-immune TG context of the KI model [18]. Hence, the membrane permeability assay was useful to explore intercellular communication in primary cultures of sensory ganglia evoked by purinergic receptor signalling possibly relevant to chronic pain conditions.

### Purinergic signalling and pore formation

R192Q KI mice express mutated Ca<sub>v</sub>2.1 channels that exhibit gain of function [13]. As a consequence, this genetic model shows enhanced excitability of TG neurons [14, 15] and larger release of neuroinflammatory modulators [16, 18]. However, the time course and the impact of soluble mediators on neuron-glia crosstalk or their role in amplifying cell responses remain incompletely understood. ATP is one of the major players of the communication between neuronal and non-neuronal cells acting on various ATP-gated receptors in a time- and concentration-dependent fashion [27]. ATP generates early ionic- and G protein-associated signalling [1], as well as slowly developing changes in membrane permeability with sustained impact on tissue inflammatory responses [28]. With respect to the latter, membrane pore permeability is evoked by prolonged activation of ATP receptors expressed by macrophages [10] and necessary to initiate inflammasome assembly, exosome release and delayed inflammatory effects [29]. The relatively long latency of the responses observed in the present study might imply slow membrane rearrangement or even indirect effects induced by agonist concentrations acting on multiple targets. It was noteworthy that, under the current experimental conditions, we did not detect any significant cell toxicity. In addition, we observed variable kinetics in the time course of the responding cells in WT or KI cultures

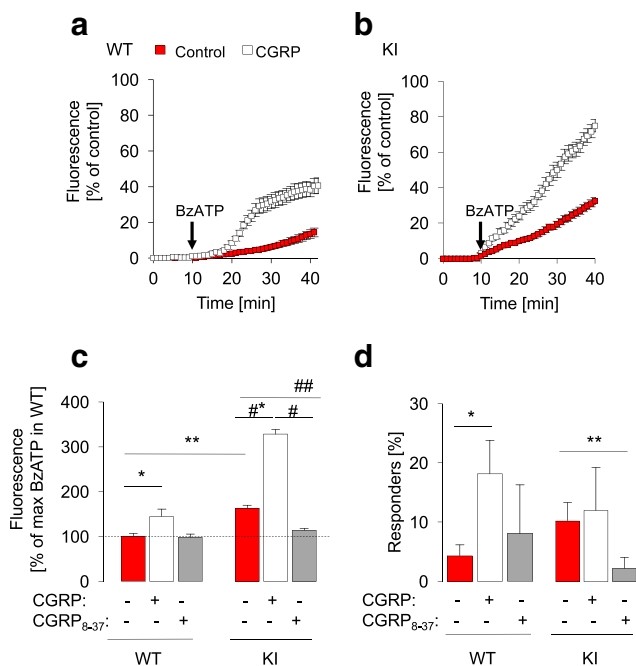


**Fig. 6** CGRP modulates membrane pore permeability in TG cultures. **a**, **b** Membrane pore permeability in TG cultures from WT (**a**) or R192Q KI (**b**) after application of BzATP (300  $\mu$ M, *arrows*), in standard conditions (control) or in cultures pre-treated with CGRP (1  $\mu$ M, 4 h). **c** Histograms quantify the fluorescence change (calculated as percentage of control samples, measured after 40 min from beginning of the recordings) in controls or after CGRP (1  $\mu$ M, 4 h) or CGRP<sub>8-37</sub> (1  $\mu$ M, 4 h) treatments. *Dashed line* indicates WT control values, taken as 100%. \* $p$  = 0.029 (WT vs WT CGRP); \*\* $p$  = 0.019 (WT vs KI control samples); # $p$  = 0.005 (KI vs KI CGRP); # $p$  = 0.037 (KI CGRP vs KI CGRP<sub>8-37</sub>), ## $p$  = 0.037 (KI vs KI CGRP<sub>8-37</sub>);  $n$  = 3. **d** Histograms quantify responding cells in each condition, measured after 20 min from beginning of the recordings. Increased fluorescent probe uptake was observed in 68/376 WT or 52/496 KI CGRP-treated cells and from 63/597 WT or 15/793 KI CGRP<sub>8-37</sub>-treated cells;  $n$  = 3; \* $p$  = 0.007 (WT vs WT CGRP), \*\* $p$  = 0.01 (KI CGRP vs KI CGRP<sub>8-37</sub>)

stimulated with different compounds that might reflect complex phenomena involving crosstalk among different pathways and/or cells inducing variations in cell membrane permeability to the fluorescent probe.

In WT cultures, a small number of cells (< 10%), characterised by ATP concentration-dependent pore formation, comprised a heterogeneous cell population (including satellite glia and inflammatory cells) likely expressing different ATP receptors. In contrast, in R192Q KI cultures, a larger number of cells responded to ATP application in accordance with higher inflammatory responses [18]. Furthermore, the steady-state response in R192Q KI culture was more intense, suggesting higher expression of P2X receptors mediating the probe uptake. The fluorescence responses evoked by BzATP application appeared to differ from the ones induced by ATP, perhaps outlining a contribution of P2Y receptors in this process. A modulatory role of P2Y receptor isoforms has been

proposed [16, 30], although their role in TG cell crosstalk requires further studies.

### P2X7 receptors of TG cultures

The persistent occupancy of agonist binding sites on certain subtypes of P2X receptors, such as P2X2, P2X4, P2X5 and P2X7 receptors [31], causes delayed formation of a cation-permeable pore that allows influx of fluorescent probes. While the mechanistic details of pore dilation remain unresolved and controversial [7], the low-affinity, slowly desensitising P2X7 receptors are the subtype first reported with this phenomenon [32]. In TG ganglia, P2X7 receptors are expressed especially by satellite glia and inflammatory cells [23], as confirmed in the present study. In R192Q KI cultures (unlike WT ones), the P2X7-preferential agonist BzATP-evoked responses prevented by the P/Q-type (Ca<sub>v</sub>2.1) specific channel blocker  $\omega$ -agatoxin IVA [14], suggesting that the larger fluorescent probe uptake phenomenon depended on the overactivity of mutated Ca<sub>v</sub>2.1 channels presumably priming the ganglion environment. Interestingly, the P2X7 receptor antagonist A-804598 as well as the large-spectrum P2X antagonist TNP-ATP had no effect on WT cultures, while they strongly inhibited responses in R192Q KI cells. Although TNP-ATP also reverses P2X4 receptor-mediated mechanical allodynia after peripheral nerve injury [33], the present data with pharmacological antagonists are broadly consistent with the outcome of P2X7 silencing in R192Q KI cultures. Our results, therefore, suggest a large contribution of P2X7 receptor-associated pore-forming mechanisms in R192Q KI. However, P2X7 receptors, particularly in WT cells, were not the sole contributors to the fluorescence signal. The present results might be accounted for by two processes, namely the existence of distinct P2X7 and P2X4 receptors or heteromeric complexes made up by a combination of such subunits. The latter possibility is compatible with the demonstration that, in inflammatory conditions, P2X4 receptors expressed in satellite glial cells can contribute to higher sensitivity to ATP [34]. The present results indicate, therefore, the novel contribution of P2X4 receptors expressed by satellite glial cells. In addition, the functional relation between P2X4 and P2X7 receptors and the occurrence of heteromeric P2X4/7 receptors has been recently detected in various tissues [35, 36], though not in TG yet. In HEK cells, recombinant heteromeric P2X4/7 receptors differentially influence ATP response, pore formation and fluorescent dye uptake with respect to expression of P2X7 alone [37–39]. Future experiments are needed to clarify these issues.

Because  $\alpha$ , $\beta$ -meATP evokes the release of endogenous ATP from neurons via a Pannexin 1-mediated mechanism [40], the application of this agonist induced a fluorescence signal that we may attribute to activation of a wider P2X receptor population following by ATP priming. The reason for the smaller effect of

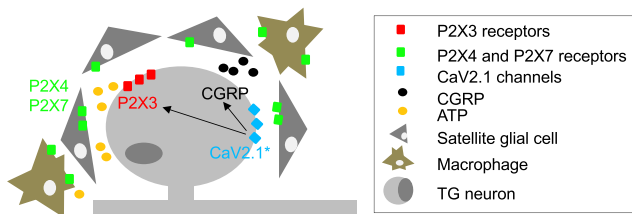


**Fig. 7** Schematic view proposing the cell arrangement underlying crosstalk among TG neurons and non-neuronal cells in KI ganglia. The diagram hypothesises facilitated release of soluble mediators such as CGRP in R192Q KI ganglia to augment P2X3 receptor-mediated responses and cell-to-cell crosstalk among neuronal and non-neuronal P2X receptors to enhance TG nociceptive signalling. Mutated R192Q CaV2.1 channels (CaV2.1\*) expressed by R192Q KI neurons are proposed to play a key role in promoting larger CGRP secretion (*black dots*), potentiation of P2X3 receptors and larger ATP release (*yellow dots*) with enhanced tissue purinergic responses. *Arrows* depict a few crucial interconnections

$\alpha,\beta$ -meATP on R192Q KI cultures remains unclear and might be possibly due to a more intense indirect contribution by P2Y receptors activated (or inactivated) by ATP [16].

### Role of CGRP in pore formation activity

Because R192Q KI cultures at baseline express a higher number of potential pore-forming cells [18] and release cytokines, ATP and CGRP [16, 18, 40], the overall higher membrane permeability in R192Q KI trigeminal cultures was consistent with the expected R192Q KI phenotype. In addition, CGRP, which is a trigger for migraine pain [41] and neuronal sensitisation [26] via immunomodulatory functions [42], potentiated fluorescence responses in a wider number of cells in R192Q KI culture rather than in WT one. The effect of endogenous CGRP was blocked by the selective inhibitor CGRP<sub>8–37</sub>, suggesting peptide receptor-mediated responses. These observations indicate the peptide role over a large population of TG cells. It is noteworthy that the facilitation of non-neuronal cell permeability by acutely applied CGRP is the only CGRP-evoked early effect detected so far in R192Q KI cultures. In summary, Fig. 7 depicts an idealised scheme for the crosstalk among sensory neurons, satellite glial cells and immune cells at the level of R192Q KI TG, involving potentiated CaV2.1 channels, enhanced release of CGRP and facilitation of P2X7 (or P2X7-like) signalling all concurring to the lowering the threshold for trigeminal pain.

### Relevance of functional crosstalk in TG cultures

In conclusion, as a consequence of amplified signalling in R192Q KI cultures, new molecular mechanisms (e.g. gene expression, splicing, subunit assembly) might emerge at the single-cell level to account for distinct pharmacological effects in R192Q KI in comparison with WT samples. This changing scenario might add further complexity to the delicate

balance regulating purinergic responses on the basis of ATP release, expression of heterogeneous receptor subtypes (with different affinity for ATP) and efficacy of ATP-hydrolysing enzymes [2, 43].

**Acknowledgments** This work was supported by EU FP7 grant EUROHEADPAIN (no. 602633) and a grant from the Slovenian Research Agency (no. ARRS J3-5503).

### Compliance with ethical standards

**Conflict of interest** Arletta Nowodworska declares that she has no conflict of interest.

Arn M. J. M. van den Maagdenberg declares that he has no conflict of interest.

Andrea Nistri declares that he has no conflict of interest.

Elsa Fabbretti declares that she has no conflict of interest.

**Ethical approval** All animal procedures were in accordance with national regulations of animal welfare and approved by the ethics committee of the International School for Advanced Studies (SISSA).

### References

- Magni G, Merli D, Verderio C, Abbraccio MP, Ceruti S (2015) P2Y2 receptor antagonists as anti-allodynic agents in acute and sub-chronic trigeminal sensitization: role of satellite glial cells. *Glia* 63: 1256–1269
- Burnstock G (2008) Purinergic signalling and disorders of the central nervous system. *Nat Rev Drug Discov* 7:575–590
- North RA, Jarvis MF (2013) P2X receptors as drug targets. *Mol Pharmacol* 83:759–769
- Inoue K, Koizumi S, Tsuda M (2007) The role of nucleotides in the neuron–glia communication responsible for the brain functions. *J Neurochem* 102:1447–1458
- Khakh BS, North RA (2012) Neuromodulation by extracellular ATP and P2X receptors in the CNS. *Neuron* 76:51–69
- Virginio C, MacKenzie A, Rassendren FA, North RA, Surprenant A (1999) Pore dilation of neuronal P2X receptor channels. *Nat Neurosci* 2:315–321
- Bean BP (2015) Pore dilation reconsidered. *Nat Neurosci* 18:1534–1535
- Virginio C, MacKenzie A, North RA, Surprenant A (1999) Kinetics of cell lysis, dye uptake and permeability changes in cells expressing the rat P2X7 receptor. *J Physiol* 519(Pt 2):335–346
- Chaumont S, Khakh BS (2008) Patch-clamp coordinated spectroscopy shows P2X2 receptor permeability dynamics require cytosolic domain rearrangements but not Panx-1 channels. *Proc Natl Acad Sci U S A* 105:12063–12068
- Browne LE, Compan V, Bragg L, North RA (2013) P2X7 receptor channels allow direct permeation of nanometer-sized dyes. *J Neurosci* 33:3557–3566
- Pelegrin P, Surprenant A (2009) Dynamics of macrophage polarization reveal new mechanism to inhibit IL-1 $\beta$  release through pyrophosphates. *EMBO J* 28:2114–2127
- Ophoff RA, Terwindt GM, Vergouwe MN, van Eijk R, Mohrenweiser H, Litt M, Hofker MH, Haan J, Ferrari MD, Frants RR (1996) A 3-Mb region for the familial hemiplegic migraine locus on 19p13.1-p13.2:

- exclusion of PRKCSH as a candidate gene. Dutch Migraine Genetic Research Group. *Eur J Hum Genet* EJHG 4:321–328
13. van den Maagdenberg AM, Pietrobon D, Pizzorusso T, Kaja S, Broos LA, Cesetti T, van de Ven RC, Tottene A, van der Kaa J, Plomp JJ, Frants RR, Ferrari MD (2004) A *Ca<sub>v</sub>1a* knockin migraine mouse model with increased susceptibility to cortical spreading depression. *Neuron* 41:701–710
  14. Nair A, Simonetti M, Birsa N, Ferrari MD, van den Maagdenberg AM, Giniatullin R, Nistri A, Fabbretti E (2010) Familial hemiplegic migraine *Ca<sub>v</sub>(v)2.1* channel mutation R192Q enhances ATP-gated P2X3 receptor activity of mouse sensory ganglion neurons mediating trigeminal pain. *Mol Pain* 6:48
  15. Hullugundi SK, Ferrari MD, van den Maagdenberg AM, Nistri A (2013) The mechanism of functional up-regulation of P2X3 receptors of trigeminal sensory neurons in a genetic mouse model of familial hemiplegic migraine type 1 (FHM-1). *PLoS One* 8:e60677
  16. Ceruti S, Villa G, Fumagalli M, Colombo L, Magni G, Zanardelli M, Fabbretti E, Verderio C, van den Maagdenberg AM, Nistri A, Abbraccio MP (2011) Calcitonin gene-related peptide-mediated enhancement of purinergic neuron/glia communication by the algogenic factor bradykinin in mouse trigeminal ganglia from wild-type and R192Q *Cav2.1* knock-in mice: implications for basic mechanisms of migraine pain. *J Neurosci* 31:3638–3649
  17. Franceschini A, Nair A, Bele T, van den Maagdenberg AM, Nistri A, Fabbretti E (2012) Functional crosstalk in culture between macrophages and trigeminal sensory neurons of a mouse genetic model of migraine. *BMC Neurosci* 13:143
  18. Franceschini A, Vilotti S, Ferrari MD, van den Maagdenberg AM, Nistri A, Fabbretti E (2013) TNF $\alpha$  levels and macrophages expression reflect an inflammatory potential of trigeminal ganglia in a mouse model of familial hemiplegic migraine. *PLoS One* 8:e52394
  19. Donnelly-Roberts DL, Namovic MT, Surber B, Vaidyanathan SX, Perez-Medrano A, Wang Y, Carroll WA, Jarvis MF (2009) [3H]A-804598 ([3H]2-cyano-1-[(1S)-1-phenylethyl]-3-quinolin-5-ylguanidine) is a novel, potent, and selective antagonist radioligand for P2X7 receptors. *Neuropharmacology* 56:223–229
  20. Mackenzie AB, Young MT, Adinolfi E, Surprenant A (2005) Pseudoapoptosis induced by brief activation of ATP-gated P2X7 receptors. *J Biol Chem* 280:33968–33976
  21. Simonetti M, Fabbro A, D'Arco M, Zweyer M, Nistri A, Giniatullin R, Fabbretti E (2006) Comparison of P2X and TRPV1 receptors in ganglia or primary culture of trigeminal neurons and their modulation by NGF or serotonin. *Mol Pain* 2:11
  22. Zhang X-F, Han P, Faltynek CR, Jarvis MF, Shieh CC (2005) Functional expression of P2X7 receptors in non-neuronal cells of rat dorsal root ganglia. *Brain Res* 1052:63–70
  23. Belzer V, Shraer N, Hanani M (2010) Phenotypic changes in satellite glial cells in cultured trigeminal ganglia. *Neuron Glia Biol* 6: 237–243
  24. Chen Y, Li G, Huang L-YM (2012) P2X7 receptors in satellite glial cells mediate high functional expression of P2X3 receptors in immature dorsal root ganglion neurons. *Mol Pain* 8:9
  25. Edvinsson L (2015) CGRP receptor antagonists and antibodies against CGRP and its receptor in migraine treatment. *Br J Clin Pharmacol* 80:193–199
  26. Fabbretti E, D'Arco M, Fabbro A, Simonetti M, Nistri A, Giniatullin R (2006) Delayed upregulation of ATP P2X3 receptors of trigeminal sensory neurons by calcitonin gene-related peptide. *J Neurosci* 26:6163–6171
  27. Petersen OH, Verkhatsky A (2016) Calcium and ATP control multiple vital functions. *Philos Trans R Soc Lond B Biol Sci* 371(1700):20150418
  28. Di Virgilio F (2007) Liaisons dangereuses: P2X(7) and the inflammasome. *Trends Pharmacol Sci* 28:465–472
  29. Karmakar M, Katsnelson MA, Dubyak GR, Pearlman E (2016) Neutrophil P2X7 receptors mediate NLRP3 inflammasome-dependent IL-1 $\beta$  secretion in response to ATP. *Nat Commun* 7: 10555
  30. Gerevich Z, Zadori Z, Müller C, Wirkner K, Schröder W, Rubini P, Illes P (2007) Metabotropic P2Y receptors inhibit P2X3 receptor-channels via G protein-dependent facilitation of their desensitization. *Br J Pharmacol* 151:226–236
  31. Rokic MB, Stojilkovic SS (2013) Two open states of P2X receptor channels. *Front Cell Neurosci* 7:215
  32. Pelegrin P, Surprenant A (2006) Pannexin-1 mediates large pore formation and interleukin-1 $\beta$  release by the ATP-gated P2X7 receptor. *EMBO J* 25:5071–5082
  33. Tsuda M, Shigemoto-Mogami Y, Koizumi S, Mizokoshi A, Kohsaka S, Salter MW, Inoue K (2003) P2X4 receptors induced in spinal microglia gate tactile allodynia after nerve injury. *Nature* 424:778–783
  34. Kushnir R, Cherkas PS, Hanani M (2011) Peripheral inflammation upregulates P2X receptor expression in satellite glial cells of mouse trigeminal ganglia: a calcium imaging study. *Neuropharmacology* 61:739–746
  35. Weinhold K, Krause-Buchholz U, Rödel G, Kasper M, Barth K (2010) Interaction and interrelation of P2X7 and P2X4 receptor complexes in mouse lung epithelial cells. *Cell Mol Life Sci* 67: 2631–2642
  36. Craigie E, Birch RE, Unwin RJ, Wildman SS (2013) The relationship between P2X4 and P2X7: a physiologically important interaction? *Front Physiol* 4:216
  37. Guo C, Masin M, Qureshi OS, Murrell-Lagnado RD (2007) Evidence for functional P2X4/P2X7 heteromeric receptors. *Mol Pharmacol* 72:1447–1456
  38. Casas-Pruneda G, Reyes JP, Pérez-Flores G, Pérez-Cornejo P, Arreola J (2009) Functional interactions between P2X4 and P2X7 receptors from mouse salivary epithelia. *J Physiol* 587:2887–2901
  39. Kawano A, Tsukimoto M, Mori D, Noguchi T, Harada H, Takenouchi T, Kitani H, Kojima S (2012) Regulation of P2X7-dependent inflammatory functions by P2X4 receptor in mouse macrophages. *Biochem Biophys Res Commun* 420:102–107
  40. Bele T, Fabbretti E (2016) The scaffold protein calcium/calmodulin-dependent serine protein kinase controls ATP release in sensory ganglia upon P2X3 receptor activation and is part of an ATP keeper complex. *J Neurochem* 138:587–597
  41. Lassen LH, Haderslev PA, Jacobsen VB, Iversen HK, Sperling B, Olesen J (2002) CGRP may play a causative role in migraine. *Cephalalgia* 22:54–61
  42. Mikami N, Matsushita H, Kato T, Kawasaki R, Sawazaki T, Kishimoto T, Ogitani Y, Watanabe K, Miyagi Y, Sueda K, Fukada S, Yamamoto H, Tsujikawa K (2011) Calcitonin gene-related peptide is an important regulator of cutaneous immunity: effect on dendritic cell and T cell functions. *J Immunol* 186:6886–6893
  43. Idzko M, Ferrari D, Eltzschig HK (2014) Nucleotide signalling during inflammation. *Nature* 509:310–317